Journal of Russian Laser Research, Volume 22, Number 1, 2001

THE RYTOV–VLADIMIRSKII PHASE AND INTERFEROMETRIC MEASUREMENTS

V. A. Andreev[1] and K. V. Indukaev[2]

[1]*P. N. Lebedev Physical Institute, Russian Academy of Sciences, Leninskii Pr. 53, Moscow 117924, Russia*
[2]*Proimpex Comtech Ltd., Suite 701, Presnenskii Val 17, Moscow 123557, Russia*
e-mail: andr@sci.lebedev.ru

Abstract

A systematic approach to the description of the topological Rytov–Vladimirskii phase was developed and a new formalism for calculating the phase in specific optical systems was constructed. This formalism uses special matrix operators that describe the variations in both the direction and polarization of optical beam as a result of its reflection and refraction at the interface between two media. The structure of the Rytov–Vladimirskii phase in optical systems with focusing lens is studied. Due to the presence of a focusing lenses, the beam trajectories are nonplanar and the Rytov–Vladimirskii phase has a singular point. At this point, the Rytov–Vladimirskii phase is not defined. It is shown that, at the singular point, the phase of a solution to the Maxwell equations is strictly defined, but its polarization is not defined. As an example, the Linnik and Mach–Zehnder interferometers are considered.

1. Introduction

At present, various optical methods of surface analysis are being intensively developed. In holography and interferometry, the phase measurements are widely used for precise investigations. On the other hand, recently, the so-called topological or geometrical phases (also referred to as the Berry phases [1–7]) have received wide recognition. In the majority of studies devoted to these phases, quantum effects are considered; however, there are also the corresponding classical analogues that arouse considerable interest as well. First of all, it is necessary to mention here the Rytov–Vladimirskii (RV) [8, 9] or spin-flop phase [10] and the Pancharantnam (P) phase [11] that arise in polarization optics. The P phase arises in the case where the polarization of a beam propagating in an optical system varies cyclically, so that the corresponding point describes a closed path on the Poincaré sphere. In this case, the initial and final states of light will differ by a phase φ_{P} defined by the solid angle subtended by that contour.

The RV phase φ_{RV} has a purely geometrical nature.

For its description, one can use an analogy with the Poincaré sphere and introduce the direction sphere. The points of this sphere correspond to directions of light rays and any trajectory of the light ray in an optical system can be represented as a contour on the direction sphere [10]. In the case where the directions of incoming and outgoing rays coincide with each other, this contour is closed. A variation in the polarization of a beam is defined by both the solid angle subtended by the contour and the initial polarization of the beam.

The RV phase can change the type of polarization, and its value depends on the initial type of polarization. Namely, if the initial beam of light had anticlockwise polarization, then, after passing the optical system, it retains its polarization, but its phase varies by the value of

$$\varphi_{\mathrm{RV}}^{L} = \Omega\,, \tag{1}$$

where Ω is a solid angle subtended by the contour on the direction sphere.

Translated from a manuscript submitted August 30, 2000.

However, if the beam has clockwise polarization, then, after passage of the optical system, it retains its polarization, but its phase varies by

$$\varphi_{\mathrm{RV}}^{R} \;=\; -\Omega\,. \tag{2}$$

The change in polarization of an arbitrary beam can be found by representing it as a linear combination of anticlockwise- and clockwise-polarized beams and using formulas (1) and (2).

Thus, the RV phase arises owing to the fact that the beam in an optical system passes along a nonplanar trajectory. There are a number of publications in which this phase was calculated for beams formed by parallel rays [12–16]. In [17], divergent light beams were considered; however, such character of their propagation was due to the configuration of the object investigated rather than because of the presence of special elements in the optical system. However, such elements, namely, lenses and nonplanar mirrors, are included in the structure of many optical devices; nevertheless, as far as we know, there have been no publications in which the RV phase brought about by such elements has been taken into account. However, these elements should be taken into account if it is the phase of a beam passed through an optical system that contains useful information. The value of the phase can be governed by various factors, and it is necessary to be able to distinguish the contributions made by different sources.

General methods for calculating the RV phase are developed in Secs. 2 and 3.

It is found [17] that, in the case of divergent light beams, there exists a direction such that the RV phase is not defined along this direction. This problem is analyzed in Sec. 4.

In Sec. 5, we discuss the procedure for taking into account the RV phase in profilometric measurements.

2. Rotation Matrices

Let us now develop a systematic approach to description and calculation of the RV phase.

We consider an optical system formed by ideal flat reflecting and refracting elements and describe the behavior of an optical beam in such a system.

We introduce a fixed laboratory coordinate system with axes X, Y, and Z. In this coordinate system, the wave vector $\vec{k}$ and polarization vector $\vec{P}$ of the optical beam after the lth reflection or refraction are given by

$$\vec{k}_l \;=\; \begin{pmatrix} k_x \\ k_y \\ k_z \end{pmatrix}_l\,, \qquad \vec{P}_l \;=\; \begin{pmatrix} P_x \\ P_y \\ P_z \end{pmatrix}_l\,. \tag{3}$$

The unit vectors $\vec{k}_l$ and $\vec{P}_l$ are orthogonal to each other. In the case of reflections and refractions, they are transformed by the same matrix M:

$$\vec{k}_n \;=\; M_n\vec{k}_0\,, \quad \vec{P}_n \;=\; M_n\vec{P}_0\,. \tag{4}$$

Here, M_n is a 3×3 unitary matrix that describes the transformations of the vectors after n reflections or refractions or both. In other words, the matrix M transforms the initial laboratory coordinate system (X, Y, Z) into a new coordinate system (X', Y', Z') linked to the space of the outgoing beam. Without loss of generality, it is possible to align the Z axis of the laboratory coordinate system with the direction of the incoming beam, so that we have

$$\vec{k}_0 \;=\; \begin{pmatrix} 0 \\ 0 \\ 1 \end{pmatrix}_0\,, \qquad \vec{P}_0 \;=\; \begin{pmatrix} P_x \\ P_y \\ 0 \end{pmatrix}_0\,.$$

In general, the polarization vector P_n has three components (4). However, choosing special coordinate systems (X', Y', Z') for which the axis Z is always directed along the beam propagation, we have

$$\vec{k}_n \;=\; \begin{pmatrix} 0 \\ 0 \\ 1 \end{pmatrix}_n , \qquad \vec{P}_n \;=\; \begin{pmatrix} P_x \\ P_y \\ 0 \end{pmatrix}_n . \tag{5}$$

Therefore, the three-dimensional polarization vector P_n can always be represented as a two-dimensional Jones vector:

$$\vec{P}_l^{\,\mathrm{J}} \;=\; \begin{pmatrix} P_x \\ P_y \end{pmatrix}_l^{\mathrm{J}} . \tag{6}$$

Let us consider the case where the direction of the outgoing beam coincides with that of the incoming beam, i.e., we have $\vec{k}_n = M_n\vec{k}_0 = \vec{k}_0$. Then it is possible to show that, for such matrices M_n, the circular-polarization vector

$$\vec{P}_0 \;=\; \begin{pmatrix} \pm i/\sqrt{2} \\ 1/\sqrt{2} \\ 0 \end{pmatrix}_0 \tag{7}$$

is an eigenvector

$$P_n \;=\; M_n P_0 \;=\; \lambda P_0 \tag{8}$$

with eigenvalues

$$\lambda \;=\; \exp(\pm\Omega). \tag{9}$$

We can define the RV phase as the phase Ω in formula (9). This phase is proportional to the solid angle subtended by the closed contour formed on the direction sphere by the motion of the tip of the wave vector. This contour represents a trajectory of a beam of light that passes through an optical system. The RV phase can also be interpreted as the angle of rotation that transforms the axes (X, Y) into the axes (X', Y'). This rotation is performed about the common axis Z that coincides with the Z and Z' axes [14]. The value of the RV phase can be determined from interference of the incoming beam P_0 with the outgoing beam P_n. In the case of circular polarization, the interference between the incoming and outgoing beams yields the signal with amplitude

$$|P_n \;+\; P_0|^2 \;=\; 2(1 \;+\cos\Omega)\,. \tag{10}$$

For a linearly polarized wave with the input polarization vector

$$\vec{P}_0 \;=\; \begin{pmatrix} 1 \\ 0 \\ 0 \end{pmatrix}_0 , \tag{11}$$

we have the output polarization vector

$$\vec{P}_n \;=\; M_n\vec{P}_0 \;=\; \begin{pmatrix} \cos\Omega \\ \sin\Omega \\ 0 \end{pmatrix}. \tag{12}$$

The wave remains linearly polarized but the polarization plane is rotated by the angle Ω in the plane (X, Y). If we detect the intensity of the outgoing beam through an analyzer

$$A \;=\; \begin{pmatrix} 1 & 0 & 0 \\ 0 & 0 & 0 \\ 0 & 0 & 1 \end{pmatrix}, \tag{13}$$

that transmits only the X component of polarization, we have

$$|A\vec{P}_n|^2 \;=\; \frac{1}{2}(1 \;+\; \cos 2\Omega). \tag{14}$$

Formula (14) has a form similar to formula (10). Thus, the use of an analyzer permits one to determine the RV phase without interferometry by using the linearly polarized light.

We see that the matrix M plays a key role in the analysis of the geometric phase RV. It has been shown [14, 15] that, in the case of reflection by ideal mirrors, the matrix M is given by

$$M \;=\; F^r_{n+1}E_nF^r_n...E_1F^r_1E_0. \tag{15}$$

Matrices E_n and F^r_n have the form

$$E_l \;=\; \begin{pmatrix} \vec{k}^i_l \\ \vec{n}_l \times \vec{k}^i_l \\ \vec{n}_l \end{pmatrix} \;=\; \begin{pmatrix} \vec{k}^i_l \\ \vec{p}^i_l \\ \vec{s}^i_l \end{pmatrix}, \qquad F^r_{l+1} \;=\; \begin{pmatrix} \vec{k}^r_{l+1} \\ \vec{n}_l \times \vec{k}^r_{l+1} \\ \vec{n}_l \end{pmatrix} \;=\; \begin{pmatrix} \vec{k}^r_{l+1} \\ \vec{p}^r_{l+1} \\ \vec{s}^r_{l+1} \end{pmatrix}. \tag{16}$$

Here, $\vec{k}^i_l$ and $\vec{k}^r_{l+1}$ are the wave vectors before and after the lth reflection, and the unit vector $\vec{n}_l$ is normal to the plane of incidence and is given by

$$\vec{n}_l \;=\; \frac{\vec{k}^i_l \times \vec{k}^r_{l+1}}{||\vec{k}^i_l \times \vec{k}^r_{l+1}||}. \tag{17}$$

Here, $||...||$ denotes the norm of the vector.

The unit vectors $\vec{p}^i_l = \vec{n}_l \times \vec{k}^i_l$ and $\vec{s}^i_l = \vec{n}_l$ define the directions parallel and normal, respectively, to the plane of incidence for the incident beam, so that the operation of the matrix E_l resolves the polarization vector P_l and the wave vector $\vec{k}_l$ into components parallel and perpendicular to the plane of incidence.

After reflection, these three components are transformed into the corresponding components defined by the unit vectors $(\vec{k}^r_{l+1}, \vec{p}^r_{l+1}, \vec{s}_{l+1})$. This process is expressed by the subsequent matrix operation F_{l+1}, and through this second operation the vectors $\vec{P}_{l+1}$ and $\vec{k}_{l+1}$ are transformed back into the components of the laboratory coordinate system. Thus, the geometry of the polarization vector P_l and the wave vector $\vec{k}_l$ at the lth mirror reflection is described by the operation of the product of two matrices $F^r_{l+1}E_l$.

In the case of refraction, we must consider the matrix F^t_{l+1} along with the matrix F^r_{l+1}. The former describes the transmitted beam and has the form

$$F^t_{l+1} \;=\; \begin{pmatrix} \vec{k}^t_{l+1} \\ \vec{n}_l \times \vec{k}^t_{l+1} \\ \vec{n}_l \end{pmatrix} \;=\; \begin{pmatrix} \vec{k}^t_{l+1} \\ \vec{p}^t_{l+1} \\ \vec{s}^t_{l+1} \end{pmatrix}. \tag{18}$$

We note that the matrix M_n is expressed only in terms of the wave vectors $\vec{k}_l$ via the matrices F^r_{l+1} and E_l rather than in terms of more direct construction parameters of the optical system such as the normal vectors of the reflecting and refracting surfaces.

In the case of normal incidence, the definitions of the plane of incidence and the $\vec{p}$ and $\vec{s}$ directions become ambiguous because the denominator in Eq. (17) vanishes. This occurs when the beam impinges normally on a wave plate and propagates through it or when the beam experiences normal reflection at the boundary surface. In this case, we maintain the same plane of incidence as that in the previous reflection or refraction and use the same normal to the plane of incidence, $\vec{n}_l = \vec{n}_{l-1}$, so that we have

$$E_l \;=\; \begin{pmatrix} \vec{k}_l^i \\ \vec{n}_{l-1} \times \vec{k}_l^i \\ \vec{n}_{l-1} \end{pmatrix} \;=\; \begin{pmatrix} \vec{k}_l^i \\ \vec{p}_l^i \\ \vec{s}_l^i \end{pmatrix}. \tag{19}$$

Since we now have $\vec{k}_l^i = \vec{k}_l^r$, the matrix $E_l F_l = I$, i.e., it becomes unitary.

Thus far we have focused our attention only on the geometric rotation of the polarization vector $\vec{P}$ and the wave vector $\vec{k}$ without considering the effect of polarization-state changes due to reflection and refraction. We now generalize formula (15) to incorporate the effect of polarization-state changes.

In the most general case, including reflection and refraction at the boundary between two media with birefringence, the polarization-state change is described by a Jones-matrix operation L:

$$L \;=\; \begin{pmatrix} L_{pp} & L_{ps} \\ L_{sp} & L_{ss} \end{pmatrix}, \tag{20}$$

where p and s stand for the components parallel (p) and normal (s) to the plane of incidence, respectively. If the two media are isotropic and homogeneous, the matrix L is reduced to a diagonal matrix with components given by the Fresnel formula. For this reason, we will refer to the polarization changes on reflection and refraction as the Fresnel effect.

Let us now recall that the operation of the matrix E_l [see Eq. (16)] resolves the polarization vector $\vec{P}_l$ into components parallel and perpendicular to the plane of incidence. Therefore, we can easily incorporate the Fresnel effect simply by inserting the following matrix between the pair of matrices $F_{l+1}^r E_l$:

$$T_l \;=\; \begin{pmatrix} 1 & 0 & 0 \\ 0 & L_{pp,l} & L_{ps,l} \\ 0 & L_{sp,l} & L_{ss,l} \end{pmatrix}. \tag{21}$$

Here, L_l denotes the Jones matrix that describes the polarization-state change on reflection or refraction at the lth surface. The matrix T will be referred to as the Fresnel matrix because it describes the Fresnel effect. Thus, we have the generalized formula

$$\tilde{M} \;=\; F_{n+1}^r T_{n+1} E_n F_n^r T_n ... E_1 F_1^r T_1 E_0, \tag{22}$$

which includes both the effects of the coordinate rotations by spin flop and the polarization-state changes on reflection and refraction.

3. Discrete Lorentz Rotations

An alternative approach to the description of the RV phase is based on the fact that electromagnetic waves with circular polarization can be represented as aggregates of photons with a certain helicity. The helicity of a photon is an eigenvalue of the operator of spin projection on its momentum. It can take the values ± 1. The helicity of a photon, as the helicity of any massless particle, is a relativistic invariant. On

the other hand, it is known that the state of a massless particle with a certain helicity is completely defined by the particle's momentum [18, 19]. If this momentum is transformed by a series of Lorentz rotations in such a manner that the final momentum coincides with the initial momentum, the initial and final states of the particle also coincide with each other to an accuracy of a certain phase. It was shown that this phase coincides with the Berry phase and, in some special cases, with the RV phase [20, 21]. We will use this construction in the case where there is a set of discrete Lorentz rotations.

Let us assume that, after a mirror reflection, the wave vector $\vec{k}_i$ is transformed into the wave vector $\vec{k}_{i+1}$:

$$\vec{k}_i \longmapsto \vec{k}_{i+1}.$$

For a linearly polarized wave an initial polarization vector P_i is transformed into a polarization vector P_{i+}:

$$\vec{P}_i \longmapsto \vec{P}_{i+1} \;=\; \vec{P}_i - 2(\vec{P}_i, \vec{k}_{i+1})\frac{\vec{k}_i + \vec{k}_{i+1}}{(\vec{k}_i + \vec{k}_{i+1})^2}\,. \tag{23}$$

Formula (23) follows from the Fresnel formulas [22].

Let us consider the sequence of n wave-vector transformations such that the final vector coincides with the initial vector:

$$\vec{k}_1 \longmapsto \vec{k}_2 \longmapsto \;\; ... \;\; \longmapsto \vec{k}_i \longmapsto \vec{k}_{i+1} \;\; ... \;\; \longmapsto \vec{k}_n \;=\; \vec{k}_1. \tag{24}$$

This sequence generates the sequence of polarization-vector transformations

$$\vec{P}_1 \longmapsto \vec{P}_2 \longmapsto \;\; ... \;\; \longmapsto \vec{P}_i \longmapsto \vec{P}_{i+1} \;\; ... \;\; \longmapsto \vec{P}_n\,. \tag{25}$$

In sequence (25), the final vector P_n does not coincide with the initial vector P_1 but is rotated relative to it at the angle Ω in the plane (X, Y). The RV phase can be defined as this angle between the vectors P_1 and P_n:

$$\varphi_{\rm RV} \;=\; \arccos(P_1, P_n). \tag{26}$$

This is an alternative definition of the RV phase.

4. Singularity of the RV Phase of Divergent Beams

In the course of investigation of divergent and convergent beams, some specific problems connected with the inhomogeneity of the RV phase arise. In the case of planar beams, this phase is constant over the cross section of a beam; however, if the beam is divergent, the RV phase experiences discontinuities whose structure depends on the properties of the specific optical system. Moreover, on the phase surface there is always a point such that at this point the RV phase is undefined. It is known that the phase of a solution to the Maxwell equations can be undefined only at the points where its amplitude is equal to zero [3, 23]. Therefore, it may appear that at the points where the RV phase is undefined the amplitude of a solution to the Maxwell equations must also be equal to zero. However, this contradicts the initial assumption that the beam amplitude is constant over its cross section. Using the exact solutions to the Maxwell equations, we will show that the phase of this solution is completely defined at each point and its amplitude is not equal to zero anywhere. The indefiniteness of the RV phase at any point leads to indefiniteness of the polarization of a solution to the Maxwell equations at this point.

In order to verify this, we will analyze the structure of the Mie solution. This exact solution describes the scattering of a plane wave by a homogeneous solid sphere [24, 25].

Let us consider a plane linearly polarized wave that propagates along the Z axis, has the polarization vector aligned with the X direction, and is incident on a sphere of radius a with permittivity ε. The strength of the incident electric field is

$$\vec{E}_i \;=\; e^{-ikz}\vec{x}. \tag{27}$$

It is known that, in spherical coordinates, every electromagnetic field can be represented in terms of scalar functions Π_1 and Π_2 that are the radial components of the Hertz vectors [24]. The function Π_1 describes all TM modes under the condition that $H_r = 0$, whereas the function Π_2 describes all TE modes providing that $E_r = 0$. Both these functions satisfy the scalar wave equations

$$(\nabla^2 \;+\; k^2)\Pi_i \;=\; 0\;, \quad i = 1, 2, \tag{28}$$

outside the sphere and

$$(\nabla^2 \;+\; \varepsilon k^2)\Pi_i \;=\; 0\;, \quad i = 1, 2,$$

inside the sphere.

In terms of the functions Π_1 and Π_2, the electric field is expressed as

$$\vec{E}_i \;=\; [\vec{\nabla}, [\vec{\nabla}, (r\Pi_1\vec{r})]] \;+\; ik[\vec{\nabla}, (r\Pi_2\vec{r})]. \tag{29}$$

In the case of plane wave (27), the functions Π_1 and Π_2 have the form [26]

$$r\Pi_1^i \;=\; \frac{1}{k^2}\sum_{n=1}^{\infty}\frac{i^{n-1}(2n+1)}{n(n+1)}\psi_n(kr)P_n^1(\cos\theta)\cos\phi\;, \tag{30}$$

$$r\Pi_2^i \;=\; \frac{1}{k^2}\sum_{n=1}^{\infty}\frac{i^{n-1}(2n+1)}{n(n+1)}\psi_n(kr)P_n^1(\cos\theta)\sin\phi\;.$$

Here, $\psi_n(x) = xj_n(x) = \sqrt{\pi x/2}J_{n+1/2}(x)$.

For scattered fields with $r > a$, we can write similar expressions containing unknown coefficients a_n and b_n:

$$r\Pi_1^i \;=\; \frac{-1}{k^2}\sum_{n=1}^{\infty}\frac{i^{n-1}(2n+1)}{n(n+1)}a_n\zeta_n(kr)P_n^1(\cos\theta)\cos\phi\;, \tag{31}$$

$$r\Pi_2^i \;=\; \frac{-1}{k^2}\sum_{n=1}^{\infty}\frac{i^{n-1}(2n+1)}{n(n+1)}b_n\zeta_n(kr)P_n^1(\cos\theta)\sin\phi\;.$$

Here, $\zeta_n(x) = xh_n^{(1)}(x) = \sqrt{\pi x/2}H_{n+1/2}^{(1)}(x)$.

For the fields inside the sphere ($r < a$), we can write similar expressions, but with other unknown coefficients c_n and d_n, i.e.,

$$r\Pi_1^i \;=\; \frac{1}{k^2\varepsilon}\sum_{n=1}^{\infty}\frac{i^{n-1}(2n+1)}{n(n+1)}c_n\psi_n(kr\sqrt{\varepsilon})P_n^1(\cos\theta)\cos\phi\;, \tag{32}$$

$$r\Pi_2^i \;=\; \frac{1}{k^2\sqrt{\varepsilon}}\sum_{n=1}^{\infty}\frac{i^{n-1}(2n+1)}{n(n+1)}d_n\psi_n(kr\sqrt{\varepsilon})P_n^1(\cos\theta)\sin\phi\;.$$

The boundary conditions for continuity of the field components $E_\theta, E_\phi, H_\theta$, and H_ϕ at the sphere $r = a$ yield expressions for the coefficients a_n and b_n:

$$a_n \;=\; \frac{\psi_n(\alpha)\psi_n'(\beta) - \sqrt{\varepsilon}\psi_n'(\alpha)\psi_n(\beta)}{\zeta_n(\alpha)\psi_n'(\beta) - \sqrt{\varepsilon}\zeta_n'(\alpha)\psi_n(\beta)}\;, \tag{33}$$

$$b_n = \frac{\psi_n'(\alpha)\psi_n(\beta) - \sqrt{\varepsilon}\psi_n(\alpha)\psi_n'(\beta)}{\zeta_n'(\alpha)\psi_n(\beta) - \sqrt{\varepsilon}\zeta_n(\alpha)\psi_n'(\beta)} .$$

Here, $\alpha = ka$ and $\beta = \sqrt{\varepsilon}ka$.

For large $r \gg a$, the scattered fields E_θ and E_ϕ have the form

$$E_\phi = -\frac{i}{kr}e^{ikr}S_1(\theta)\sin\phi , \quad E_\theta = \frac{i}{kr}e^{ikr}S_2(\theta)\cos\phi , \tag{34}$$

$$S_1(\theta) = \sum_{n=1}^{\infty}\frac{2n+1}{n(n+1)}[a_n\pi_n(\cos\theta) + b_n\tau_n(\cos\theta)] ,$$

$$S_2(\theta) = \sum_{n=1}^{\infty}\frac{2n+1}{n(n+1)}[a_n\tau_n(\cos\theta) + b_n\pi_n(\cos\theta)] .$$

Here,

$$\pi_n(\cos\theta) = \frac{P_n^1(\cos\theta)}{\sin\theta} , \quad \tau_n(\cos\theta) = \frac{d}{d\theta}P_n^1(\cos\theta) .$$

One can see from formulas (34) that a Maxwell-equation solution describing the scattered wave has a well-defined phase at all points of the space. Polarization of the solution is constant along each direction $\vec{r}$. If we calculate the limit of polarization for $\theta \to 0$ and $\phi = \text{const}$, it can be seen that this limit depends on the spherical angle ϕ. Thus, we find that polarization of the solutions (34) is not defined for $\theta = 0$.

This indefiniteness of the polarization is caused by the indefiniteness of the RV phase of divergent beams.

Let us now consider examples of specific interferometers.

5. The Linnik Interferometer

This section is devoted to calculation of the RV phase existing in a Linnik interferometer. This device is frequently used as a profilometer [27]; therefore, it is necessary to be able to separate the contribution to the phase of the probing beam arising owing to the path traversed by this beam from the contribution connected with the nonplanarity of its trajectory, i.e., from the RV phase.

The schematic diagram of the interferometer is shown in Fig. 1.

It includes a lens L_0, a beamsplitter BS, two mirrors M_1 and M_2, and also two lenses L_1 and L_2 mounted in front of mirrors M_1 and M_2. These lenses are frequently referred to as microobjectives. If lenses L_1 and L_2 were absent, it would be the usual Michelson interferometer. It is for such an interferometer that we shall carry out an initial calculation of the distribution of the RV phase, and then we shall show that the addition of microobjectives in the diagram changes nothing.

The device also contains a source of radiation I and a detector D, where beams of light from different channels are mixed.

We describe the vector $\vec{n}$ that specifies the direction of the beam of light using a spherical system of coordinates, i.e., using the angles θ and φ. The angle θ is measured from the positive direction of the Z axis and the angle φ is the angle between the vector $\vec{n}$ component in the XY plane and positive direction of the X axis in the counterclockwise direction.

The Z axis is directed along the optical axis of the lens L_0 from left to right, the X axis is perpendicular to the plane of the mirror M_2 and is directed upwards, and the Y axis lies in the plane of the mirror M_2 and is perpendicular to the plane of the drawing in Fig. 1.

The beam of light generated by the source I is incident on the lens L_0. All rays of the beam are parallel to the Z axis. The lens L_0 transforms the parallel beam into a converging one and directs it to the beamsplitter

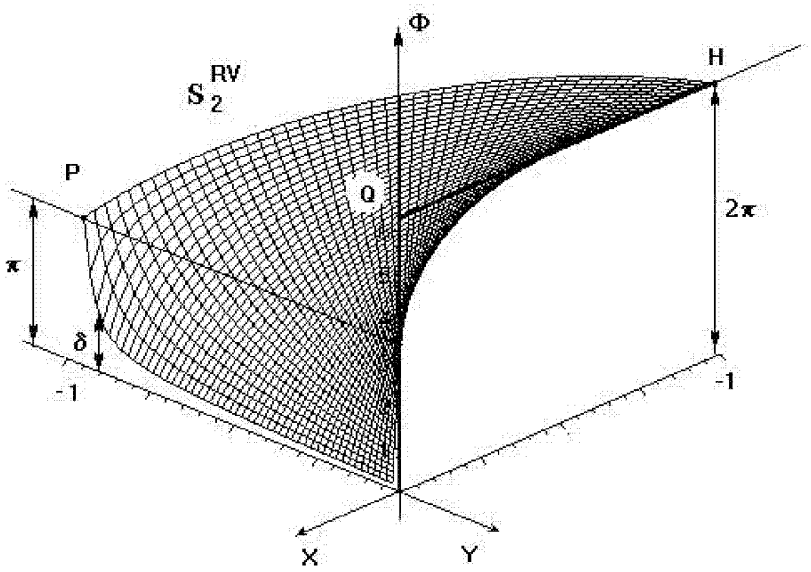

Fig. 1. Schematic diagram of a Linnik interferometer.

BS. At the beamsplitter, the initial beam is divided into two beams. One of the beams passes through the beamsplitter BS, is incident on the mirror M_1, is reflected from it, comes back to the beamsplitter BS and, having reflected from it, falls on the detector D. The second beam falls on the mirror M_2, is reflected from it, passes through the beamsplitter BS and falls on the detector D, where it is mixed up with the first beam.

Optical elements of the interferometer are mounted in such a manner that the rays of the first and second beams striking the same point of the plane of the detector D have identical directions. However, it is not important whether the focuses of the lens L_0 are in front of the mirrors M_1 and M_2 or behind them; it is only important that both of them be on the same side of these mirrors.

Let us now describe the motion of light beams in the interferometer in terms of vectors of their directions.

1. The first beam corresponds to reference beams. The vectors of its directions form the following sequence:

$$(0,\ 0,\ 1)_1^{\mathrm{I}} \ \rightarrow \ (\sin\theta\sin\varphi,\ \sin\theta\cos\varphi,\ \cos\theta)_1^{\mathrm{L_0}} \ \rightarrow \tag{35}$$

$$(-\cos\theta,\ \sin\theta\cos\varphi,\ \sin\theta\sin\varphi)_1^{\mathrm{M_1}} \ \rightarrow \ (\cos\theta,\ \sin\theta\cos\varphi,\ \sin\theta\sin\varphi)_1^{\mathrm{BS}} \ .$$

Here, the subscript is the channel number, and the superscript specifies an optical element in the channel in which the beam with the corresponding direction vector is formed.

2. The second beam of light corresponds to probing beams. The vectors of its directions form the following sequence:

$$(0,\ 0,\ 1)_2^{\mathrm{I}} \ \rightarrow \ (\sin\theta\sin\varphi,\ \sin\theta\cos\varphi,\ \cos\theta)_2^{\mathrm{L_0}} \ \rightarrow \tag{36}$$

$$(\sin\theta\sin\varphi,\ \sin\theta\cos\varphi,\ -\cos\theta)_2^{\mathrm{BS}} \ \rightarrow \ (\cos\theta,\ \sin\theta\cos\varphi,\ \sin\theta\sin\varphi)_2^{\mathrm{M_2}} \ .$$

Let us plot vectors (35) and (36) on the direction sphere and join the next points in these sequences by arcs of great circles. The figure arising from it is shown in Fig. 2. It corresponds to the case where the beam of

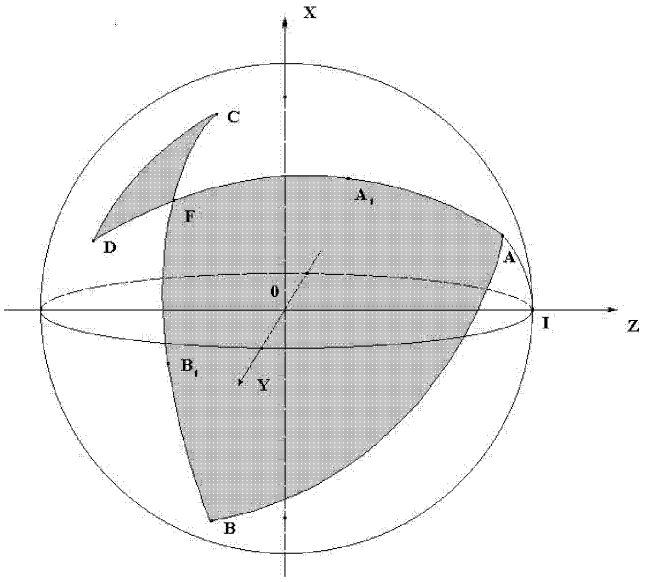

Fig. 2. The pattern of trajectories of beams on the direction sphere in a Linnik interferometer.

light after passing the lens L_0 is characterized by a vector having positive components along the OX and OY axes. For other beams, these components of their vectors may be negative.

Let us now describe all points in Fig. 2. The point I with coordinates

$$(0, 0, 1) \tag{37}$$

corresponds to the beam that comes from the left to the lens L_0 and runs along the OZ axis. After passing the lens L_0, the beam refracts, and the vector of its direction acquires the coordinates

$$(\ \sin\theta \sin\varphi,\ \sin\theta \cos\varphi,\ \cos\theta\ ). \tag{38}$$

This vector is represented on the direction sphere by the point A. The points I and A are joined by an arc of a great circle. After that, the beam A falls on the beamsplitter BS, where it is divided into two beams: the reference and probing ones. The reference beam passes through the beamsplitter BS, without changing direction, falls on the mirror M_1, is reflected from it, and acquires the direction

$$(\ -\cos\theta,\ \sin\theta \cos\varphi,\ \sin\theta \sin\varphi\ ). \tag{39}$$

The point D on the direction sphere corresponds to this direction. It is easy to see that beams (37), (38), and (39) lie in the same plane; therefore, their corresponding points I, A, and D lie on the same arc of the great circle. Having reflected from a mirror M_1, the beam D propagates to the beamsplitter BS, is reflected from it, and acquires the direction C:

$$(\ \cos\theta,\ \sin\theta \cos\varphi,\ \sin\theta \sin\varphi\ ). \tag{40}$$

We can see that the broken line $IADC$ formed on the direction sphere by two segments of arcs of the great circle, ID and DC, corresponds to the trajectory of the reference beam.

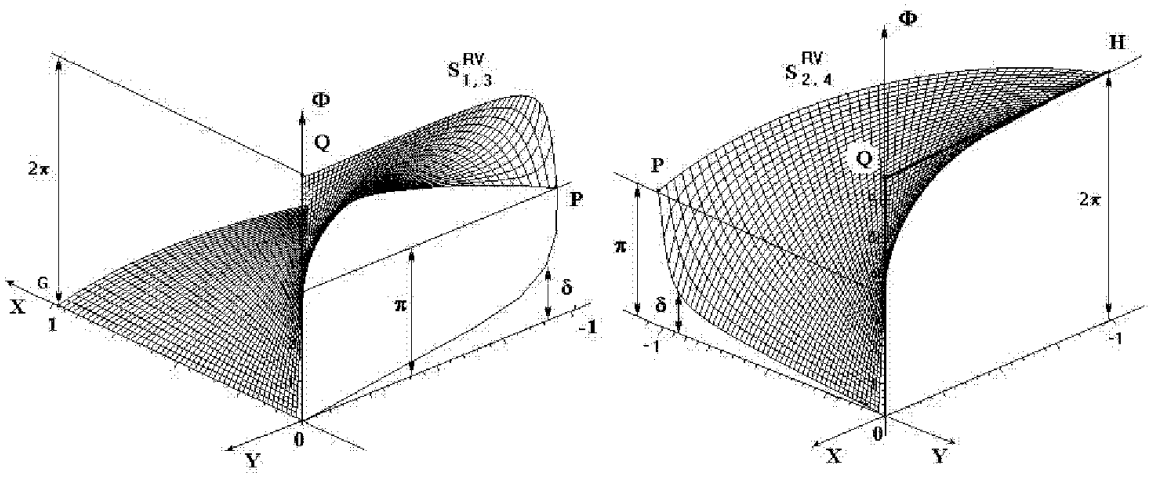

Fig. 3. The Rytov–Vladimirskii phase surface for a Linnik interferometer: parts of the S^{RV} surface located in the first (S^{RV_1}) and third (S^{RV_3}) quadrants of the XY plane (a) and parts of the S^{RV} surface located in the second (S^{RV_2}) and fourth (S^{RV_4}) quadrants of the XY plane (b).

Let us now describe the trajectory of the probing beam. This beam arises from the initial-beam half that does not pass through the beamsplitter BS but is reflected from it. After such reflection, the probing beam begins to propagate along the direction

$$(\sin\theta \sin\varphi,\ \sin\theta \cos\varphi,\ -\cos\theta\ ). \tag{41}$$

The point B on the direction sphere corresponds to this direction. After that, the beam falls on the mirror M_2, is reflected from it, and propagates along the direction

$$(\cos\theta,\ \sin\theta \cos\varphi,\ \sin\theta \sin\varphi\ ). \tag{42}$$

The point C on the direction sphere corresponds to direction (42). Thus, on the direction sphere the end of the trajectory of the probing beam coincides with the end of the reference-beam trajectory.

The arc AD crosses the arc BC at the point F.

The trajectories of the reference and probing beams form a figure consisting of two triangles, ABF and FCD, on the direction sphere. In order to find the RV phase, it is necessary to calculate the areas of these triangles.

The result of calculation based on formula (42) is shown in Fig. 3.

The distribution of the RV phase for the anticlockwise polarized wave forms the surface S^{RV} above the plane XY. On this plane, we set the Cartesian coordinates with the axes X and Y. Each point of this surface with coordinates (x, y) corresponds to the beam that crosses the lens L_0 at a point with the same coordinates. After the light beam crosses the plane of the lens at the point (x, y), the direction of its propagation will be set by vector (38). The angle θ is defined only by the distance $\rho = \sqrt{x^2 + y^2}$ of the point (x, t) from the origin of coordinates, and the angle φ coincides with the angle ψ of this point in polar coordinates. For this

reason, in order to describe the phase-surface structure, we use the polar coordinates (ρ, ψ) on the XY plane. We measure the angle ψ from the positive direction of the X axis to the negative direction of the Y axis, i.e. clockwise. We choose the scale on the X and Y axes in such a manner that the radius ρ on the phase surface in Fig. 3 varies from 0 to 1. This corresponds to a change in the angle θ from 0 to $\pi/4$, i.e., the angle $\theta = \pi/4$ corresponds to the value $\rho = 1$. The angle ψ varies from 0 up to 2π.

The surface S^{RV} has the property of symmetry

$$S^{\mathrm{RV}}(\psi + \pi) \; = \; S^{\mathrm{RV}}(\psi). \tag{43}$$

For this reason, we may restrict ourselves to the description of the surface S^{RV} only within the boundaries

$$0 \le \rho \le 1 \; , \quad 0 \le \psi \le \pi. \tag{44}$$

Let us present the value of the phase φ_{RV} on the X axis:

$$\varphi_{\mathrm{RV}} \; = \; 2\pi, \quad \text{if} \;\; 0 < \rho \le 1 \; , \;\; \psi = 0, \tag{45}$$

$$\varphi_{RV} \; = \; 0, \quad \text{if} \;\; 0 < \rho \le 1 \; , \;\; \psi = \pi.$$

Now we describe the value of the phase φ_{RV} on the circle $\rho = r$.

If $r = 1$, the phase φ_{RV} increases linearly from $\varphi_{\mathrm{RV}}(1, 0) = 0$ to $\varphi_{\mathrm{RV}}(1, \pi) = 2\pi$; in this case, $\varphi_{\mathrm{RV}}(1, \pi/2) = \pi$:

$$\varphi_{RV}(1, \psi) \; = 2\psi.$$

However, if $r = a < 1$, the phase φ_{RV} increases steadily from $\varphi_{\mathrm{RV}}(1, 0) = 0$ to $\varphi_{\mathrm{RV}}(1, \pi) = 2\pi$, but at the point $(a, \pi/2)$ it varies by a jump. Thus, on the Y axis, the phase φ_{RV} has a discontinuity whose magnitude is equal to 2π at the point $(0, 0)$; this vanishes at the point $(1, \pi/2)$.

The part of the surface S^{RV} corresponding to the boundaries $0 \le \psi \le \pi/2$ is represented in Fig. 3a; we designate this part as S_1^{RV}. The part of the surface S^{RV} corresponding to the boundaries $\pi/2 \le \psi \le \pi$ is represented in Fig. 3b; we designate this part as S_1^{RV}. The segment $0Q$ and the point P are common for these two parts of the surface S^{RV}. The boundary $0P$ of the surface S_2^{RV} in Fig. 3b corresponds to the line $0P$ in Fig. 1a.

The values of the RV phase for angles $\psi > \pi$ can be found using symmetry relation (43).

Thus, for $0 < \rho < 1$, the given surface has the form of a four-thread screw. Its pitch is close to (somewhat smaller than) 8π if ρ is close to zero, and steadily decreases, tending to 4π with increasing ρ. At the instant when the parameter ρ attains the value of $\rho = 1$, the four-thread screw transforms into a two-thread screw with a pitch of 4π.

Such a form is typical of the RV phase surface for the Linnik interferometer.

Up to this point, we calculated the RV phase without taking into account the lenses L_1 and L_2 installed in front of the mirrors M_1 and M_2, i.e., we actually considered a conventional Michelson interferometer. Let us now take these lenses into account.

In the case of the reference beam, the light passes through the beamsplitter BS, hits the lens L_1, and is refracted by it. Before hitting the lens L_1, the beam of light was characterized by vector (38); as a result of the refraction, the angle θ of a direction vector changes as $\theta \; \rightarrow \; \theta'$, whereas the angle φ remains unchanged. Therefore, after the refraction, the vector (38) will be transformed as follows:

$$(\; \sin\theta \sin\varphi, \; \sin\theta \cos\varphi, \; \cos\theta \;) \; \rightarrow \; (\; \sin\theta' \sin\varphi, \; \sin\theta' \cos\varphi, \; \cos\theta' \;). \tag{46}$$

After reflection from the mirror M_1, the light beam (46) acquires the direction

$$(\; -\cos\theta', \; \sin\theta' \cos\varphi, \; \sin\theta' \sin\varphi \;), \tag{47}$$

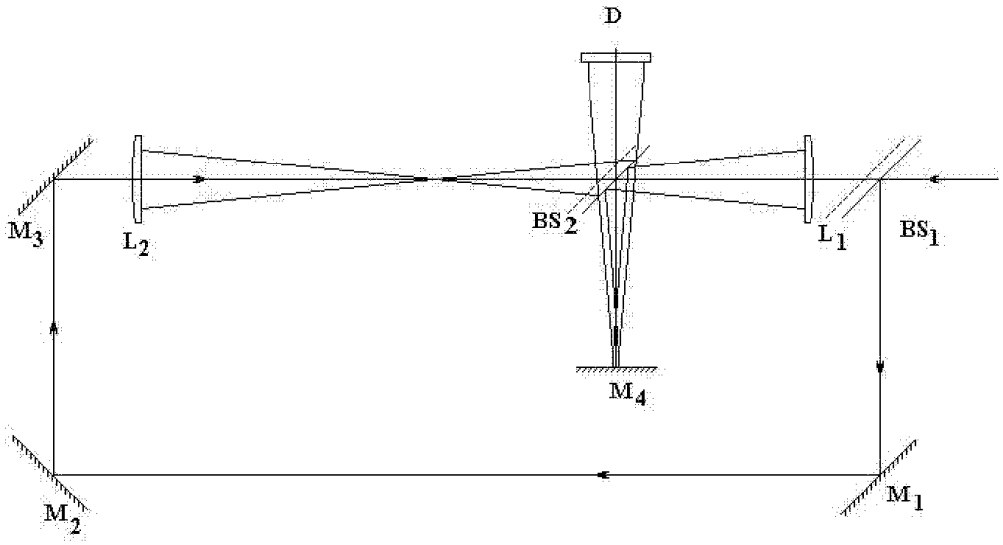

Fig. 4. Schematic diagram of a Mach–Zehnder interferometer.

and, after passing the lens L_1 in the opposite direction, it is described by vector (39). It is easily seen that the points A and D corresponding to directions (38) and (39) and the points P and Q corresponding to directions (46) and (47) lie on the same arc of the great circle. Therefore, the area of the figure on the direction sphere corresponding to trajectories of the probing and reference beams in the interferometer does not vary when lenses L_1 and L_2 are added to the optical system. In view of this, the value of the corresponding RV phase does not vary either.

It follows from the above reasoning that, if there are two consecutive directions of a light beam $\vec{n}_1$ and $\vec{n}_2$ forming the plane N_{12}, any additional change in the direction of the beam in the interval between $\vec{n}_1$ and $\vec{n}_2$ does not affect the RV phase if the directions of these changes lie in the plane N_{12}.

6. The Mach–Zehnder Interferometer

We now come to the analysis of the Mach–Zehnder interferometer. The schematic diagram of the device is shown in Fig. 4.

It includes two beamsplitters, BS_1 and BS_2, four mirrors, M_1, M_2, M_3, and M_4, and two lenses, L_1 and L_2. The device also includes a source of radiation I and a detector D; in this detector, the beams from different channels are mixed.

We describe the vector $\vec{n}$ that specifies the direction of the light beam using the same spherical system of coordinates as in the case of the Linnik interferometer.

The light beam generated by the source I falls on the beamsplitter BS_1. All rays of the beam are parallel to the Z axis. At the beamsplitter, the initial beam is divided into two beams. Of these, the beam that is reflected from the beamsplitter BS_1 forms the reference beam. It passes first the plane contour, consecutively reflecting from the mirrors M_1, M_2, and M_3, and falls on the lens L_2. The lens L_2 transforms the parallel beam into a converging one and directs it at the beamsplitter BS_2. Then, having reflected from it, the referece

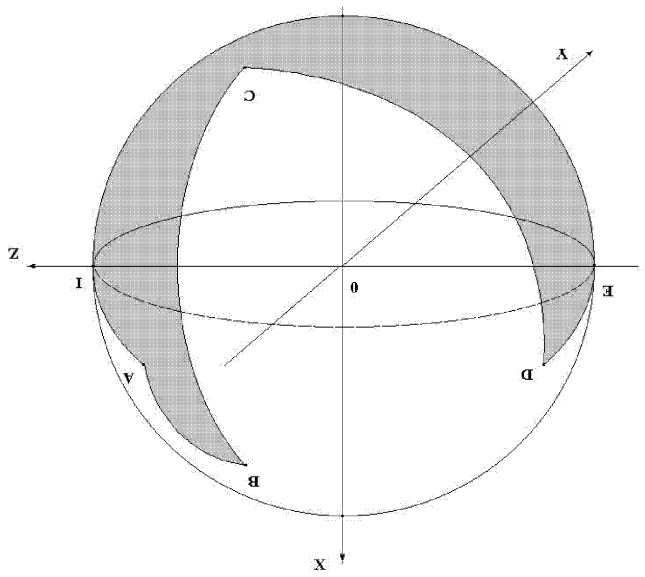

Fig. 5. The pattern of the trajectories of beams' on the direction sphere for a Mach–Zehnder interferometer.

beam hits the detector D.

The second half of the beam forms the probing beam. It passes through the beamsplitter BS_1 and falls on the lens L_1. This lens transforms the parallel beam into a converging one and directs it at the beamsplitter BS_2. Then, having reflected from it, the probing beam falls on the mirror M_4, is reflected from it, comes back to the beamsplitter BS_2, and, passing through it, hits the detector D, where it is mixed with the first beam.

The mirror M_4 can be used as a substrate for an object under investigation. That is why we refer to the second beam as the probing beam.

Let us now describe the motion of light beams in a Mach–Zehnder interferometer in terms of vectors of their directions and indicate the corresponding points on the direction sphere in Fig. 5.

1. The first beam of light corresponds to reference rays. The vectors of its directions form the following sequence:

$$\begin{gathered}(\,0,\,0,\,-1\,)_1^{\mathrm{I}} \;\rightarrow\; (\,-1,\,0,\,0\,)_1^{\mathrm{BS_1}} \;\rightarrow \\ (\,0,\,0,\,-1\,)_1^{\mathrm{M_1}} \;\rightarrow\; (\,1,\,0,\,0\,)_1^{\mathrm{M_2}} \;\rightarrow\; (\,0,\,0,\,1\,)_1^{\mathrm{M_3}} \;\rightarrow \\ (\,\sin\theta\cos\varphi,\,\sin\theta\sin\varphi,\,\cos\theta\,)_1^{\mathrm{L_2}} \;\rightarrow\; (\,\cos\theta,\,\sin\theta\sin\varphi,\,\sin\theta\cos\varphi\,)_1^{\mathrm{M_1}}\,.\end{gathered} \tag{48}$$

Here, the subscript specifies the number of the channel, and the superscript corresponds to an optical element in the channel that forms the beam with the corresponding direction vector. The corresponding points on the directions sphere are

$$I \;\rightarrow\; G \;\rightarrow\; I \;\rightarrow\; H \;\rightarrow\; E \;\rightarrow\; D \;\rightarrow\; C\,.$$

2. The second light beam corresponds to probing rays. The vectors of its directions form the following sequence:

$$\begin{gathered}(\,0,\,0,\,-1\,)_1^{\mathrm{I}} \;\rightarrow\; (\,0,\,0,\,-1\,)_1^{\mathrm{BS_1}} \;\rightarrow\; (\,\sin\theta\cos\varphi,\,\sin\theta\sin\varphi,\,-\cos\theta\,)_1^{\mathrm{L_1}} \;\rightarrow \\ (\,-\cos\theta,\,\sin\theta\sin\varphi,\,\sin\theta\cos\varphi\,)_1^{\mathrm{BS_2}} \;\rightarrow\; (\,\cos\theta,\,\sin\theta\sin\varphi,\,\sin\theta\cos\varphi\,)_1^{\mathrm{M_4}}\,.\end{gathered} \tag{49}$$

The corresponding points on the direction sphere are given by

$$I \ \rightarrow \ I \ \rightarrow \ A \ \rightarrow \ B \ \rightarrow \ C \, .$$

Let us plot the vectors in sequences (48) and (49) on the direction sphere and join the neighboring points in these sequences by arcs of great circles. The figure $IABCDEI$ arising from it is shown in Fig. 5. In order to find the RV phase for the Mach–Zehnder interferometer, we should calculate the area of this figure.

The result of calculation is illustrated in Fig. 6a and 6b.

The distribution of the RV phase for a circularly polarized wave forms the surface S^{RV} above the plane XY. As in the case of the Linnik interferometer, the surface S^{RV} has the property of symmetry:

$$S^{\mathrm{RV}}(\psi + \pi) \ = \ S^{\mathrm{RV}}(\psi). \tag{50}$$

For this reason, we can restrict ourselves to the description of the surface S^{RV} only within the boundaries

$$0 \leq \rho \leq 1 \, , \quad 0 \leq \psi \leq \pi. \tag{51}$$

We now present the value of the phase φ_{RV} on the X axis.

At the point $(\rho = 1, \psi = \pi)$ the phase is equal to

$$\varphi_{RV}(1, \pi) = \pi.$$

If the parameter ρ decreases from $\rho = 1$ to $\rho = 0$ and the equality $\psi = \pi$ remains valid, the phase φ_{RV} decreases steadily from $\varphi_{\mathrm{RV}}(1, \pi) = \pi$ to $\varphi_{\mathrm{RV}}(0, \pi) = 0$.

At the point $(0, \pi)$, φ_{RV} changes drastically by 2π. At the point $(0, 0)$, the phase φ_{RV} takes the value of $\varphi_{\mathrm{RV}}(0, 0) = 2\pi$ and then steadily decreases to $\varphi_{\mathrm{RV}}(1, 0) = \pi$.

On the circle $\rho = 1$, the phase φ_{RV} is constant and equal to π:

$$\varphi_{\mathrm{RV}}(1, \psi) = \pi.$$

In the course of anticlockwise motion along the circle $\rho = r < 1$, the phase φ_{RV} steadily increases from the value $\pi - \Delta(r)$ at the point $(r, 0)$ to the value $\pi + \Delta(r)$ at the point (r, π). The function $\Delta(r)$ steadily increases with decreasing r from $\Delta(1) = 0$ to $\Delta(0) = 2\pi$. Thus, at the points $(r, 0)$ and (r, π) of the X axis, the phase φ_{RV} has a discontinuity whose magnitude is equal to $2\Delta(r)$. On the Y axis, the phase φ_{RV} is constant and equal to π, taking into account that it is not defined at the point $(0, \pi/2)$:

$$\varphi_{\mathrm{RV}}(r, \pi/2) = \pi.$$

Thus, outside $0 < \rho < 1$, the given surface has the form of a two-thread screw. Its pitch is close to 4π when ρ is close to zero, and steadily decreases, tending to 0 with increasing ρ. At the instant the parameter ρ attains the value $\rho = 1$, the four-thread screw transforms into a smooth circle.

Such a form has the RV phase surface for the Mach–Zehnder interferometer. Its two projections are represented in Fig. 6a and 6b.

7. The RV Phase and Profilometric Measurements

Let us now discuss the question of how one can take into account the above results in the case of profilometric measurements.

Let us assume that, for some reason, the probing beam passing an optical system acquires, in relation to a reference beam, some additional phase δ, which is independent of polarization of the beam. This can be

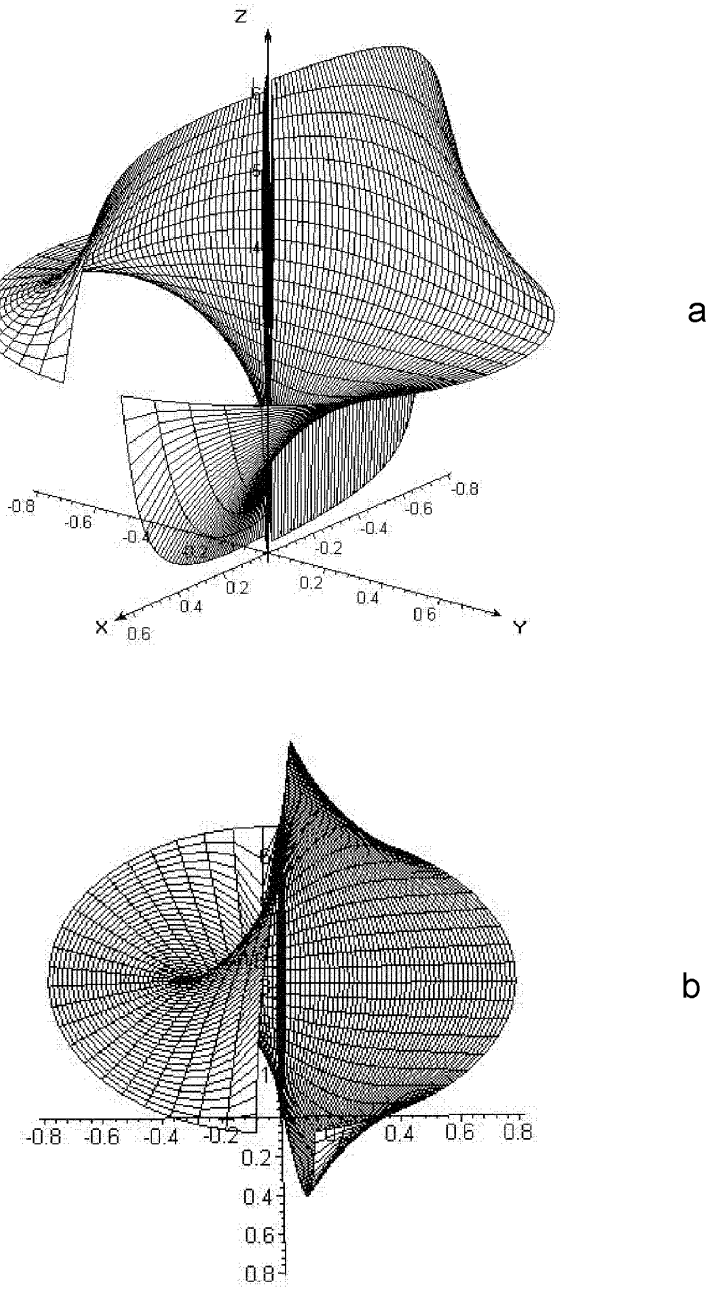

Fig. 6. Two projections of the Rytov–Vladimirskii phase surface for a Mach–Zehnder interferometer.

caused, for example, by the difference in optical paths between the reference and probing beams. We shall call it a dynamic phase.

Let us consider separately the anticlockwise polarized, clockwise polarized, and linearly polarized waves.

1. The Jones vector of an anticlockwise-polarized wave has the form

$$E_{\mathrm{LF}} \;=\; \frac{1}{\sqrt{2}}\begin{pmatrix}1\\ i\end{pmatrix}. \tag{52}$$

After the entire optical path is completed, the difference of the phases between the reference and probing beams is $\delta+\Omega$, i.e., the sum of the dynamic and RV phases. The wave incident on the detector is a superposition of the reference and probing waves:

$$E^1_{\mathrm{LF}} \;+\; E^2_{\mathrm{LF}} \;=\; \frac{1}{2\sqrt{2}}\left[\begin{pmatrix}1\\ i\end{pmatrix} \;+\; \begin{pmatrix}1\\ i\end{pmatrix} e^{i(\delta+\Omega)}\right]. \tag{53}$$

The square of its amplitude has the form

$$|E^1_{\mathrm{LF}} \;+\; E^2_{\mathrm{LF}}|^2 \;=\; \frac{1}{2}[1 \;+\; \cos(\delta+\Omega)]. \tag{54}$$

2. For a clockwise-polarized wave, the Jones vector has the form

$$E_{\mathrm{RT}} \;=\; \frac{1}{\sqrt{2}}\begin{pmatrix}1\\ -i\end{pmatrix}. \tag{55}$$

Now, after the optical path is completed, the difference of the phases between the reference and probing beams takes the form $\delta-\Omega$, i.e., it is the difference of the dynamic phase and the RV phase. The wave incident on the detector is a superposition of the reference and probing waves:

$$E^1_{\mathrm{RT}} \;+\; E^2_{\mathrm{RT}} \;=\; \frac{1}{2\sqrt{2}}\left[\begin{pmatrix}1\\ -i\end{pmatrix} \;+\; \begin{pmatrix}1\\ -i\end{pmatrix} e^{i(\delta-\Omega)}\right]. \tag{56}$$

Now the square of the incident-wave amplitude has the form

$$|E^1_{\mathrm{RT}} \;+\; E^2_{\mathrm{RT}}|^2 \;=\; \frac{1}{2}[1 \;+\; \cos(\delta-\Omega)]. \tag{57}$$

3. Let us now consider a linearly polarized wave. It can be represented as the sum of the clockwise- and anticlockwise-polarized waves:

$$E_{\mathrm{LN}} \;=\; \begin{pmatrix}1\\ 0\end{pmatrix} \;=\; \frac{1}{\sqrt{2}}(E_{\mathrm{LF}} \;+\; E_{\mathrm{RT}}) \;=\; \frac{1}{2}\left[\begin{pmatrix}1\\ i\end{pmatrix} \;+\; \begin{pmatrix}1\\ -i\end{pmatrix}\right]. \tag{58}$$

The wave incident on the detector is given by

$$E^1_{\mathrm{LN}} \;+\; E^2_{\mathrm{LN}} \;=\frac{1}{4}\left[\begin{pmatrix}1\\ i\end{pmatrix} \;+\; \begin{pmatrix}1\\ -i\end{pmatrix} \;+\; \begin{pmatrix}1\\ i\end{pmatrix} e^{i(\delta+\Omega)} \;+\; \begin{pmatrix}1\\ -i\end{pmatrix} e^{i(\delta-\Omega)}\right]. \tag{59}$$

The square of its amplitude has the form

$$|E^1_{\mathrm{LN}} \;+\; E^2_{\mathrm{LN}}|^2 \;=\; \frac{1}{2}(1 \;+\; \cos\delta\cos\Omega). \tag{60}$$

Let us assume that we use the interferometer as a profilometer [27]. In this case, we determine the position of a point at the surface by maximizing the signal amplitude and modulating the dynamic phase δ. Then it follows from formulas (54), (57), and (60) that, for a clockwise-polarized wave, the constructed image of a point of the surface is displaced in relation to its true position by a value proportional to the RV phase Ω. For an anticlockwise-polarized wave, the image of a point of the surface is displaced by the same distance but in the opposite direction. If the wave is linearly polarized, the image of a point of the surface is not displaced.

The existence of this effect was demonstrated experimentally in [16] in measuring the shape of the surface of latex balls using a profilometer with light of various polarizations. This presence of this effect means that the RV phase must be taken into account (among other effects) when dealing with polarized light and interpreting the phase shift Δ between the beams passing different paths in an optical system. Thus, the presence of information on the structure of the RV phase related only to the optical system itself, i.e., the phase surfaces (see Figs. 3 and 6), allows one to separate the contributions to the shift Δ from the device and from the object under investigation. In fact, such a phase surface is a characteristic of each specific optical device and should be included in its certificate. It is also useful to know the shape of this surface because, in this case, it is possible to choose the appropriate smooth areas on it for better performance of the device.

Since the RV phase depends on polarization of a beam, whereas the dynamic phase and the P phase are independent of polarization, one can carry out a series of measurements with light of various polarizations to separate them from each other. A device [28–30] combining the characteristics of both an ellipsometer and a profilometer is based on this principle.

Acknowledgments

This study was performed within the framework of the Project "Modulational and Interferometric Microscopy" carried out by the AMPHORA LLC company.

Appendix

In this Appendix, we give analytical formulas for calculating the RV phase surfaces that are illustrated in Figs. 3 and 6. The corresponding figures on the direction spheres are divided into several spherical triangles and after that the areas of these triangles are calculated using the formula [31]

$$S_\Delta \;=\; 4\arctan\left[\tan\frac{L}{2}\tan\left(\frac{L-a}{2}\right)\tan\left(\frac{L-b}{2}\right)\tan\left(\frac{L-c}{2}\right]\right)^{\frac{1}{2}}. \qquad (A1)$$

Here, a, b, and c are the sides of a triangle and $L = \frac{1}{2}(a+b+c)$ is its semiperimeter. In our case, the side of a triangle is a segment of an arc of a great circle; therefore, its length is equal to the angle subtended by this segment. The value of this angle can be found by calculating the scalar product of radius vectors that form this angle.

1) The Linnik interferometer.

The analytical formula for the phase φ_{RV} as a function of two spherical angles θ and φ has the form of the sum of formulas (A1) for two spherical triangles, ABF and FCD, in Fig. 2.

The expression for the area of the triangle ABF has the form

$$S_{ABF} \;=\; 4\arctan\left(\sqrt{\tan(Q_1+Q_2)\tan(-Q_1+Q_2)\tan^2(Q_1)}\right), \qquad (A2)$$

where

$$Q_1 \;=\; \frac{1}{4}\arccos(-\sin 2\theta\cos\varphi + \sin^2\theta\sin^2\varphi)\;,$$

$$Q_2 \;=\; \frac{1}{2}\arccos\left(\frac{\sin\theta\cos\varphi+\sin\theta\sin\varphi\tan\varphi-\cos\theta}{\sqrt{2+\tan^2\varphi}}\right)\,.$$

The expression for the area of the triangle FCD has the form

$$S_{FCD} \;=\; \varphi_{\rm RV}(\theta,\varphi) \;=\; 4\arctan\left(\sqrt{\tan(Q_1'+Q_2')\tan(-Q_1'+Q_2')\tan^2(Q_1')}\right), \qquad (A3)$$

where

$$Q_1' \;=\; \frac{1}{4}\arccos(\sin 2\theta\cos\varphi+\sin^2\theta\sin^2\varphi)\,,$$

$$Q_2' \;=\; \frac{1}{2}\arccos\left(\frac{\sin\theta\cos\varphi+\sin\theta\sin\varphi\tan\varphi+\cos\theta}{\sqrt{2+\tan^2\varphi}}\right)\,.$$

Thus,

$$\varphi_{\rm RV}(\theta,\varphi) \;=\; S_{ABF} \;+\; S_{FCD}. \qquad (A4)$$

Let us determine the RV phase (A4) on the Z axis. To this end, we calculate the limit

$$\lim_{\theta\to 0}\varphi_{\rm RV}(\theta,\varphi) \;=\; 8\arctan\left[(\tan q_1\tan q_2)^{\frac{1}{2}}\tan\left(\frac{\pi}{8}\right)\right]. \qquad (A5)$$

Here,

$$q_1 \;=\; \left[\frac{\pi}{8}+\frac{1}{2}\arccos\left(\frac{1}{\sqrt{2+\tan^2\varphi}}\right)\right],$$

$$q_2 \;=\; \left(-\frac{\pi}{8}+\frac{1}{2}\arccos\left(\frac{1}{\sqrt{2+\tan^2\varphi}}\right)\right].$$

We see that the value of the RV phase (A4) at the Z axis depends on the angle φ, in other words, on the direction along which the Z axis is approached. Therefore, the RV phase is not defined at the Z axis. It is just the singular point which was discussed in Sec. 4.

2) The Mach–Zehnder interferometer.

In order to calculate the RV phase for a Mach–Zehnder interferometer, one must determine the area of the figure $IABCDEI$ shown in Fig. 5. In order to do so, we divide it into five triangles and calculate their areas separately. The summarized expression has the form

$$S_{IABCDEI} \;=\; S_1+S_2+S_3+S_4+S_5. \qquad (A6)$$

Here,

$$S_1 \;=\; 4\arctan\left(\sqrt{\tan Q_1^1\tan Q_2^1\tan Q_3^1\tan Q_4^1}\right),$$

where

$$Q_1^1 \;=\; \left[\frac{1}{4}\theta+\frac{1}{4}\arccos(\sin\theta\cos\varphi)+\frac{1}{4}\arccos(\sin^2\theta\sin^2\varphi)\right],$$

$$Q_2^1 \;=\; \left[-\frac{1}{4}\theta+\frac{1}{4}\arccos(\sin\theta\cos\varphi)+\frac{1}{4}\arccos(\sin^2\theta\sin^2\varphi)\right],$$

$$Q_3^1 \;=\; \left[\frac{1}{4}\theta-\frac{1}{4}\arccos(\sin\theta\cos\varphi)+\frac{1}{4}\arccos(\sin^2\theta\sin^2\varphi)\right],$$

$$Q_4^1 \;=\; \left[\frac{1}{4}\theta + \frac{1}{4}\arccos(\sin\theta\cos\varphi) - \frac{1}{4}\arccos(\sin^2\theta\sin^2\varphi)\right];$$

$$S_2 \;=\; 4\arctan\left(\sqrt{\tan Q_1^2 \tan Q_2^2 \tan Q_3^2 \tan Q_4^2}\right),$$

where

$$\begin{aligned}
Q_1^2 \;&=\; \frac{1}{4}\arccos(\sin 2\theta\cos\varphi + \sin^2\theta\sin^2\varphi) + \frac{1}{4}\arccos(\sin^2\theta\sin^2\varphi)\\
&\quad + \frac{1}{4}\arccos(-\cos^2\theta + \sin^2\theta\sin^2\varphi + \sin^2\theta\cos^2\varphi),\\
Q_2^2 \;&=\; -\frac{1}{4}\arccos(\sin 2\theta\cos\varphi + \sin^2\theta\sin^2\varphi) + \frac{1}{4}\arccos(\sin^2\theta\sin^2\varphi)\\
&\quad + \frac{1}{4}\arccos(-\cos^2\theta + \sin^2\theta\sin^2\varphi + \sin^2\theta\cos^2\varphi),\\
Q_3^2 \;&=\; \frac{1}{4}\arccos(\sin 2\theta\cos\varphi + \sin^2\theta\sin^2\varphi) - \frac{1}{4}\arccos(\sin^2\theta\sin^2\varphi)\\
&\quad + \frac{1}{4}\arccos(-\cos^2\theta + \sin^2\theta\sin^2\varphi + \sin^2\theta\cos^2\varphi),\\
Q_4^2 \;&=\; \frac{1}{4}\arccos(\sin 2\theta\cos\varphi + \sin^2\theta\sin^2\varphi) + \frac{1}{4}\arccos(\sin^2\theta\sin^2\varphi)\\
&\quad - \frac{1}{4}\arccos(-\cos^2\theta + \sin^2\theta\sin^2\varphi + \sin^2\theta\cos^2\varphi);
\end{aligned}$$

$$S_3 \;=\; 4\arctan\left(\sqrt{-\tan Q_1^3 \tan Q_2^3 \cot Q_3^3 \tan Q_4^3}\right),$$

where

$$\begin{aligned}
Q_1^3 \;&=\; \frac{1}{4}\arccos\left(\sin\theta\cos\varphi + \frac{1}{8}\pi + \frac{1}{4}\theta\right),\\
Q_2^3 \;&=\; \frac{1}{4}\arccos\left(-\sin\theta\cos\varphi + \frac{1}{8}\pi + \frac{1}{4}\theta\right),\\
Q_3^3 \;&=\; \frac{1}{4}\arccos\left(\sin\theta\cos\varphi + \frac{3}{8}\pi + \frac{1}{4}\theta\right),\\
Q_4^3 \;&=\; \frac{1}{4}\arccos\left(\sin\theta\cos\varphi + \frac{1}{8}\pi - \frac{1}{4}\theta\right);
\end{aligned}$$

$$S_4 \;=\; 4\arctan\left(\sqrt{\tan Q_1^4 \tan Q_2^4 \tan Q_3^4 \tan Q_4^4}\right),$$

where

$$\begin{aligned}
Q_1^4 \;&=\; \frac{1}{4}\arccos(-\sin 2\theta\cos\varphi + \sin^2\theta\sin^2\varphi) + \frac{1}{4}\pi - \frac{1}{4}\arccos(\sin\theta\cos\varphi) + \frac{1}{4}\theta,\\
Q_2^4 \;&=\; -\frac{1}{4}\arccos(-\sin 2\theta\cos\varphi + \sin^2\theta\sin^2\varphi) + \frac{1}{4}\pi - \frac{1}{4}\arccos(\sin\theta\cos\varphi) + \frac{1}{4}\theta,\\
Q_3^4 \;&=\; \frac{1}{4}\arccos(-\sin 2\theta\cos\varphi + \sin^2\theta\sin^2\varphi) - \frac{1}{4}\pi + \frac{1}{4}\arccos(\sin\theta\cos\varphi) + \frac{1}{4}\theta,
\end{aligned}$$

$$Q_4^4 \;=\; \frac{1}{4}\arccos(-\sin 2\theta\cos\varphi + \sin^2\theta\sin^2\varphi) + \frac{1}{4}\pi - \frac{1}{4}\arccos(\sin\theta\cos\varphi) - \frac{1}{4}\theta;$$

$$S_5 \;=\; 4\arctan\left(\sqrt{-\tan Q_1^5 \tan Q_2^5 \tan Q_3^5 \cot Q_4^5}\right),$$

where

$$\begin{aligned}
Q_1^5 &= \frac{3}{8}\pi - \frac{1}{4}\arccos(\sin\theta\cos\varphi) + \frac{1}{4}\theta,\\
Q_2^5 &= \frac{3}{8}\pi - \frac{1}{4}\arccos(\sin\theta\cos\varphi) - \frac{1}{4}\theta,\\
Q_3^5 &= -\frac{1}{8}\pi + \frac{1}{4}\arccos(\sin\theta\cos\varphi) + \frac{1}{4}\theta,\\
Q_4^5 &= \frac{5}{8}\pi - \frac{1}{4}\arccos(\sin\theta\cos\varphi) + \frac{1}{4}\theta.
\end{aligned}$$

References

1. M. V. A. Berry, *Proc. Roy. Soc. A*, **392**, 45 (1984).
2. B. Simon, *Phys. Rev. Lett.*, **51**, 2167 (1983).
3. M. V. A. Berry, *Phys. Today*, **12**, 34 (1990).
4. V. A. Andreev, A. B. Klimov, and P. B. Lerner, *Pis'ma Zh. Éksp. Teor. Fiz.*, **50**, 63 (1989).
5. V. A. Andreev, A. B. Klimov, and P. B. Lerner, *Europhys. Lett.*, **12**, 101, (1990).
6. S. I. Vinitskii, V. L. Derbov, V. M. Dubovik, and Yu. P. Stepanovskii, *Usp. Fiz. Nauk*, **160**, 1 (1990).
7. D. N. Klyshko *Usp. Fiz. Nauk*, **163**, 189 (1993).
8. S. M. Rytov, *Dokl. Akad. Nauk SSSR*, **28**, 263 (1938); English translation in: B. Markovski and S. I. Vinitsky (Eds.), *Topological Phases in Quantum Theory*, World Scientific, Singapore (1989), p. 6.
9. V. V. Vladimirsky, *Dokl. Akad. Nauk SSSR*, **31**, 222 (1941); English translation in: B. Markovski and S. I. Vinitsky (Eds.), *Topological Phases in Quantum Theory*, World Scientific, Singapore (1989), p. 11.
10. H. Jiao, S. R. Wilkinson, R. Chiao, and H. Nathel, *Phys. Rev. A*, **39**, 3479 (1989).
11. S. Pancharatnam, *Proc. Ind. Acad. Sci., Ser. A*, **44**, 247 (1956).
12. A. Bergamin, G. Cavagnero, and G. Mana, *J. Mod. Opt.*, **39**, 2053 (1992).
13. P. Hariharan, K. J. Larkin, and M. Roy, *J. Mod. Opt.*, **41**, 663 (1994).
14. A. V. Tavrov, T. Kawabata, Y. Miyamoto, et al., *J. Opt. Soc. Am. A*, **16**, 919 (1999).
15. A. V. Tavrov, T. Kawabata, Y. Miyamoto, et al., *J. Opt. Soc. Am. A*, **17**, 154 (2000).
16. A. V. Tavrov, T. Kawabata, Y. Miyamoto, et al., *Opt. Lett.*, **25**, N7, 1 (2000).
17. V. A. Andreev, A. V. Tavrov, D. V. Ublinsky, et al., *Bulletin of the Lebedev Physics Institute*, No. 5/6, 44 (1996).
18. S. S. Schweber, *An Introduction to Relativistic Quantum Field Theory*, Row & Peterson, New York (1961).
19. A. I. Akhiezer and V. B. Berestetskii, *Quantum Electrodynamics* [in Russian], Nauka, Moscow (1981).
20. I. Bialynicki-Birula and S. Bialynicki-Birula, *Phys. Rev. D*, **35**, 2383 (1987).
21. T. F. Jordan, *J. Math. Phys.*, **28**, 1759 (1987).
22. M. Born and E. Wolf, *Principles of Optics*, Pergamon, Oxford (1968).
23. N. B. Baranova and B. Ya. Zel'dovich, *Zh. Éksp. Teor. Fiz.*, **80**, 1789 (1982).
24. A. Ishimaru, *Wave Propagation and Scattering in Random Media*, Vol. 1, Academic Press, New York (1978).
25. M. Kerker, *The Scattering of Light*, Academic Press, New York (1978).

26. J. Stratton, *Electromagnetic Theory*, McGraw-Hill, New York (1941).
27. Yu. V. Kolomiitsov, *Interferometers* [in Russian], Mashinostroenie, Leningrad (1976).
28. A. V. Tavrov, V. A. Andreev, and D. V. Ublinsky, *Opt. Tekh.*, No. 3(7), 15 (1995).
29. A. Tavrov, V. Andreev, D. Ublinsky, et al., *Proc. SPIE*, **2778**, 1072 (1996).
30. V. A. Andreev, K. V. Indukaev, A. V. Tavrov, et al., Patent RF No. 2029976, class G02B 21/00 (1995).
31. G. A. Korn and T. M. Korn, *Mathematical Handbook*, McGraw-Hill, New York (1968).